Impacts of Low-Head Dam Construction and Removal with Little Channel Sediment Storage: Case Study from the Maury River, Virginia

Chantal Iosso and David Harbor

Abstract

Dam removal projects are becoming more frequent as awareness of the negative ecological consequences increases and dams begin to fail. However, due to the potential threats of post-removal channel migration, bank erosion, and sediment pollution, it is important to develop case studies that can help water managers and others predict the potential responses under different geologic and climate conditions. The Jordan's Point Dam, a low-head 19th-century dam on the Maury River in Rockbridge County, Virginia, was removed in May 2019. The Maury River drains 1280 km^2 of the southern Shenandoah Valley underlain by carbonates, but carries coarse-grained material from the adjacent Valley and Ridge sandstones. We use a combination of aerial and bank photography, cross section measurements, and sediment sampling to characterize the response of the stream to dam removal. Floods that occur in any season both raised floodplain heights and transported fine sediments and likely gravels and cobbles through the impounded reach during dam emplacement, resulting in little fine sediment storage in the channel behind the dam. After dam removal, water level drop in the 2-km-long impoundment revealed several types of material. The largely steep and muddy banks have failed in isolated reaches and are compacting where underlain by organic deposits The bed is characterized by dipping limestone bedrock covered by cobbles in newly exposed riffles and sand draped cobbles in pools. Due to the coarse, cobble structure of most of the thalweg, initial channel changes and sediment removal were minimal, involving some mud being cut from steep exposed banks and shifting of sand in exposed riffles. We evaluate the hypotheses that the coarse bed structure either developed in response to high flows through the modified reach or that is simply a fossilized pre-dam condition; in either case, larger floods are required to mobilize bed sediment in the impounded reach. We model sediment transport capacity of the stream prior to dam removal and post-removal under increasing flow using HEC-RAS. We also approximate the depth of legacy sediment stored in the floodplains and its susceptibility to erosion.

Introduction

Waterways in the United States currently contain over 2.5 million dams, affecting every watershed larger than 2000 square kilometers (Cannatelli & Curran 2012). Many of these dams, constructed in the 1960s, now need costly repair or removal (Gartner, Magilligan, & Renshaw, 2015). In addition, increased awareness of the negative consequences of dams emphasize the need for removal. Dams can form ecological barriers in the water, preventing passage and thus gene flow of aquatic species like fish (Roberts et al. 2007). Dams also reduce habitat complexity by eliminating the riffle, run, and glide features of unaffected rivers, therefore removing habitats needed for certain species to spawn or feed (DGIF 2018). Additionally, dams can present hazards to humans, such as when a teenager drowned beneath Jordan's Point dam (hereafter "the dam") in Rockbridge County in 2006 (DGIF 2018). Removing dams also adds recreational value to rivers as it provides easier passage for boaters (DGIF 2018). Because of the increased awareness, many dams have been or are in the process of being removed, which is a trend that will likely continue (Borroughs et al. 2009).

Removal of dams can result in channel migration, erosion, and sediment pollution (Wildman & MacBroom 2004). Understanding and predicting stream morphology change is critical to minimizing ensuing erosion and sediment pollution and avoiding the need of costly remediation measures later. A large volume of legacy sediment stored in floodplains while dams are in place can erode after dam removal, introducing fine sediment into the stream. Erosion of the legacy sediments in the bank could result in water quality pollution, as legacy sediment and higher nutrient levels within negatively impact the delicate environment of the Chesapeake Bay (Hupp et al. 2013). However, stream response to dam removal varies by site and is not currently predictable from previous models or studies (Pizzuto 2002). Rather, site specific analysis must be undertaken. Due to the increased rate of dam removal, studying river responses in a variety of environments is critical to inform future removal practices. As a low-head dam with minimal fine sediment storage in the channel behind the dam, the Jordan's Point Dam merits additional research. Few previous studies have examined stream response to removal of low-head dams; in these studies, responses vary based on factors including proximity to other dams, sediment storage, and others (Kim & Toda 2018; Fencl et al. 2015). Additionally, new research indicates that reservoirs behind low-head dams and weirs may only be 25% full (Pearson & Pizzuto 2015),

because D_{50} to D_{90} material moves over the dam in floods (Pearson & Pizzuto 2015; Peeters et al. 2020; Casserly et al. 2020). Given multiple new studies documenting movement of cobbles over, and minimal fine sediment storage behind, low-head dams, this bedload condition may be common among other low-head dams. Thus, modeling morphological changes along the Maury after the removal of the dam will increase understanding of channel responses to dam removal in similar, understudied systems.

We use a combination of aerial, bank, and bed imagery, hydraulic modeling, and channel and bank sediment sampling to characterize the nature of the former impoundment and further to predict the response of the Maury River to dam emplacement and removal. We seek to understand the way channel morphology and channel and bank sediment accumulation and distribution changed with the dam in place, and how channel form, bedload, and bank erosion will change after dam removal.

Site Description

Maury River: The Maury River drains 1280 square kilometers at the dam in Lexington, VA. Sediment sources include Cambrian and Ordovician carbonates (commonly dolomites and marls) of the southern Shenandoah Valley which contribute to the suspended load of the river, and Silurian sandstones from the Alleghany Ridges which make up most of the channel cobbles (Wilkes et al. 2007). Land within this area is 77% forested, 18% agriculture (mostly cattle pasture), and 5% developed (USGS Stream Stats 2019) and receives and average of 114.3 centimeters of precipitation annually (USGS Stream Stats 2019).

The Maury River is a mixed alluvial-bedrock river exhibiting pool-riffle morphology. In most areas, the Maury has ingrown meanders flanked by terraces in a generally narrow floodplain corridor within bedrock walls. Although much of the river has been at least intermittently impounded by crib dams or locks (more than 25 structures over 50 kilometers of the stream surrounding the Jordan's Point Dam) (Trout 1991), undammed reaches are characterized by riffles with large cobble island or bank-attached bars with a thin cobble cover over bedrock in the channel and exposed bedrock in pools. In the impoundment, cobbles, draped with sand in pools, dominate the channel thalweg and overlie limestone bedrock ledges that are occasionally exposed. Sandy, natural levees also line portions of the channel. The average gradient of six kilometers surrounding the impounded area is 0.00267.

Jordan's Point Dam: The Jordan's Point dam, initially wooden, was installed as early as 1806 on the Maury River in Lexington, Virginia to power a mill, although this functionality ceased long before the dam's removal (Kalbian & Pezzoni 2019). During the first hundred years following its construction, it breached at least once before and once after 1840 during flood events, and was replaced both times. In 1911, the modern concrete dam was built on top of an un-breached crib dam (Kalbian & Pezzoni 2019) (figure 1). This low-head, run-of-the-river concrete dam measuring three meters high and 56 meters across created a two-kilometer impoundment upstream (DGIF 2018). Due to extensive cracks that would have necessitated costly repairs, the Virginia Department of Game and Inland Fisheries removed it in May 2019 (figure 2). Little fine sediment was stored in the channel behind the dam. Floods, that can occur in any season, most likely stored sand and finer sediment on the surrounding heightened floodplains. The removal of the dam resulted in a large water level drop which exposed steep, muddy-sand banks.

Figure 1. Historic image of the Jordan's Point Dam.

Figure 2. Image of the Jordan's Point Dam being removed in May 2019. Timbers of the older, un-breached crib dam in front of which the concrete dam was built are visible.

Methods

Channel Characterization and Hydraulic Modeling

Eighteen cross sections were collected along nearly 2 kilometers of the Maury River (figure 3). The downstream-most cross section is located approximately 60 meters downstream of the remains of the Jordan's Point Dam. Cross sections were extended up to the floodplain or higher surface on either side wherever possible. Cross section locations were selected to best capture bed morphology changes (transitions between pools and riffles, bed gradient changes, etc.), resulting in areas of higher cross section density in areas that change morphology over short stream distances. We used a Topcon total station and recorded horizontal distance, vertical difference, and angle to each point, including a benchmark, to locate cross sections. Benchmark locations and cross sections are marked by either an X on rock or a labeled stake, depending on the location, to facilitate repeat cross sections. A Trimble Geo7X GPS was used to locate benchmarks with centimeter error by leaving the GPS in each location for at least 15 minutes. We added additional, non-surveyed points on each cross section from the Rockbridge-area LIDAR (USGS 2020) to extend cross section coverage across the entire floodplain.

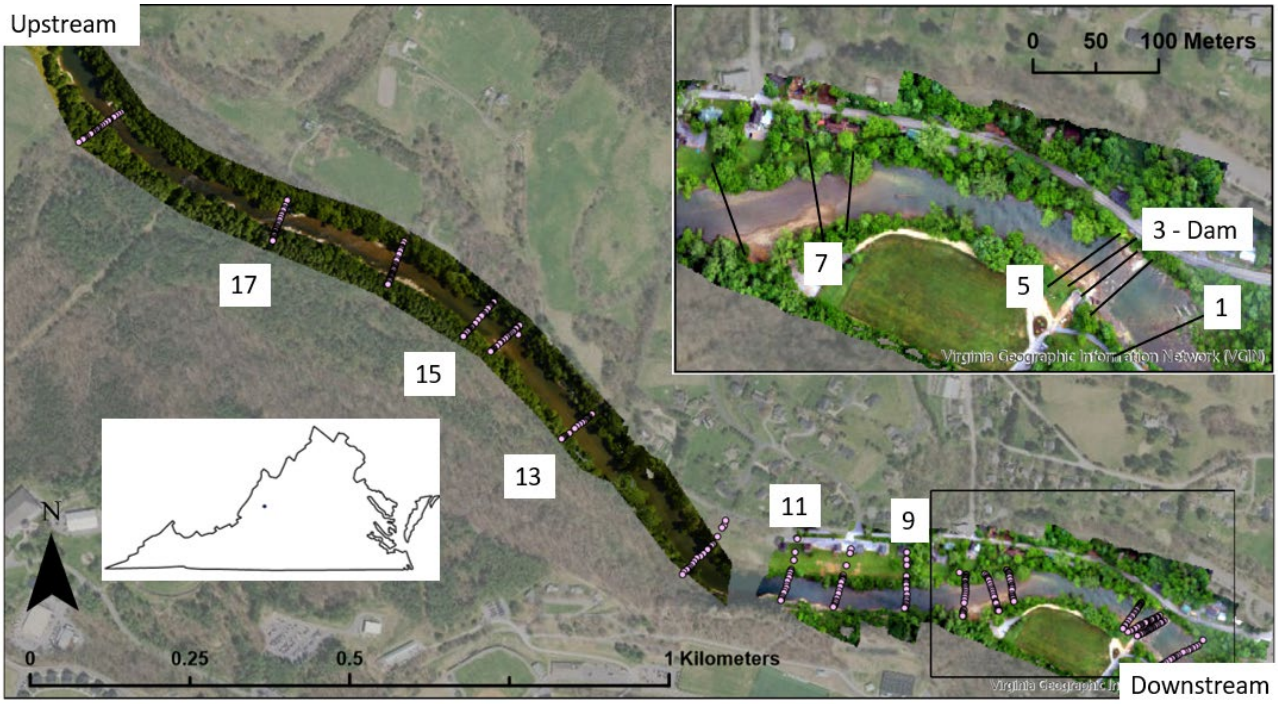

Figure 3. Aerial imagery of the area of the Maury River impounded by the Jordan's Point Dam (lower right corner). Cross sections are identified with purple dots, and odd-numbered cross sections are labelled. The small box in the bottom left corner identifies the location of the Maury River in Virginia. Cross section three is along the remnants of the dam, and cross section 17 marks the top of the low-water impoundment.

We input XYZ cross section data into HEC-RAS, a hydraulic modeling software (https://www.hec.usace.army.mil/software/hec-ras/download.aspx). Cross sections were numbered such that the lowest numbers corresponded to the farthest downstream; all cross section points were input from river left to river right. We traced the riverbanks and central flow-path in HEC-RAS, intersecting all cross sections, using imported satellite imagery as a visual aid. Necessary conditions for running hydraulic modeling through this software include local flood recurrence data, boundary conditions, Manning's n of the floodplain and channel, and channel and overbank distances.

To approximate the flood recurrence at the dam, annual peak discharge for the Maury River near Rockbridge Baths (about 15 km upstream of the dam, USGS gauge 02021500) was downloaded for the period of record, 1929 to 2017. We ranked data by discharge (rank of 1 is the highest discharge, N is the total number of years and the rank corresponding to the lowest peak discharge during the collection period) and calculated flood recurrence (R, years) for each discharge using the formula R = (N+1)/M, where M is the rank of that discharge. To account for skewness in the distribution of floods, discharges corresponding to each flood probability (Q_R) were calculated using the log Pearson Type 3 distribution

$$\log Q_R = \frac{\sum \log Q}{N} + K\sigma$$

(OSU Streamflow Tutorial). We calculated standard deviation (σ) and the Pearson skewness following OSU Streamflow Tutorial, and linearly interpolated the corresponding K values of 2-, 5-, 10-, 50-, and 100-year floods for that skewness from the conversion table in England et al. 2019.

This regression was used to determine flood discharges corresponding with 2-, 5-, 10-, 50-, and 100-year probability floods, which were input as flow conditions for HEC-RAS. Conversion of flood discharge at the gauge to flow at the study site was accomplished using the ratio of drainage area.

We ran models using steady-flow analysis, so only downstream boundary conditions were required for the reach. We calculated normal depth, approximated by the average gradient of the riverbed throughout the reach (distance along river channel divided by total elevation change of the thalweg).

We compared Maury River channel photos and bed characteristics to images from the Barnes (1967) study to visually identify the best match of Manning's n value. For the majority of the reach, the cobble-bed structure with thin, localized sand drapes best matched photos corresponding with n values of 0.032. Upstream, where bedrock ledges are more prominent and exposed along portions of the channel, we selected 0.043 for n. Floodplain n values were calculated based on Arcement & Schneider, 1989 by adding together n values for the base material, irregularity of the surface, amount of obstructions, and level of vegetation corresponding to that surface (table 1).

Table 1. Manning's n calculations for floodplains and surfaces along the Maury River.

	Base N	N1 irregularity	N3 obstructions	N4 vegetation	Total
Grassy fields	0.02	0.006	0.002	0.01	0.038
Forested areas	0.02	0.01	0.05	0.06	0.14

Using satellite imagery in ArcMap base maps as a guide, we measured distances from upstream cross sections to the next one down along the center of the channel, right bank, and left bank for input to HEC-RAS.

To verify the accuracy of the hydraulic model, I compared the elevation of the two-year recurrence interval flood modeling (with dam) with recorded footage during a September 28, 2018 flood in Lexington that closely corresponded with a two-year flood. At several locations, the model elevations closely matched the water levels of the videos (figure 4).

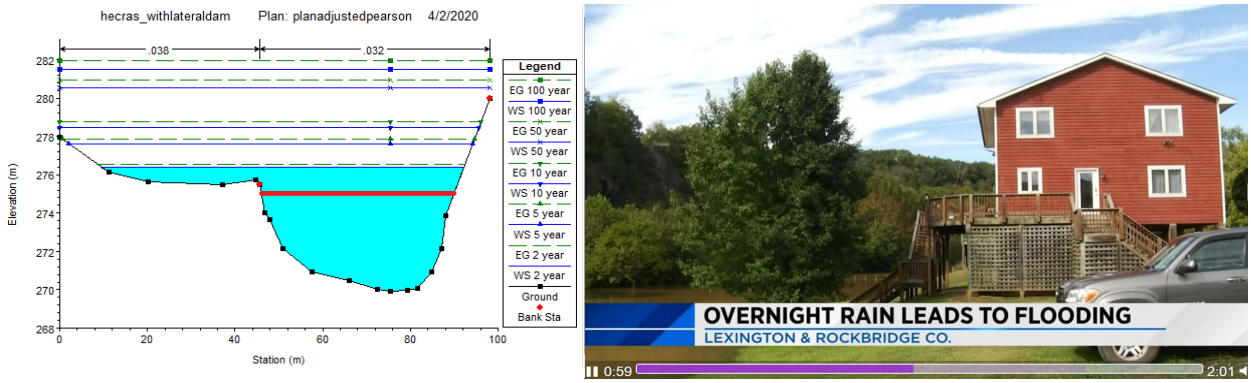

Figure 4. HEC-RAS model results for cross section nine during a two-year flood with the dam in place, compared to videos from approximately a two-year flood at the same location on September 28th, 2018 recorded by WSLS: https://www.wsls.com/news/2018/09/28/rockbridge-county-faces-flooding-issues-after-heavy-overnight-rains/ (at 0:59). HEC-RAS imagery is oriented looking downstream, while the video is taken looking upstream. In both, water is near the base of the steeper slope before the houses. The thick red line denotes the modeled elevation of a two-year flood after dam removal.

Channel Sediment Analysis

We characterized bed armor in all exposed riffles (cross sections 3, 4, 7, 14, 15, 16, and 17), by measuring cobbles exposed at the cross section. At least 50 sediment samples were collected per cross section; we repeated river crossings in the same area to obtain more samples to meet the minimum 50 when necessary. Approximately every half meter across the river, I sampled the first cobble I touched without looking and recorded b-axis size in half-phi (mm) interval using a gravelometer. Areas with bedrock lining the bottom of the channel were not sampled.

We characterized bulk sediment size distribution by weight at cobble bars and banks recently exposed by the water level drop following dam removal. In each location, we first removed the armoring clasts from an approximately 400 square centimeter area. Then, we used a shovel to collect the sediment underneath the cleared area into a bucket. Any clast that touched the shovel was sampled to avoid bias.. Then, sediment was sieved into phi intervals from 64 to 2 mm. Clasts larger than 64 mm were measured with a gravelometer. We weighed each interval, with the difference between the total weight and the sum of the other portions representing the weight of material finer than 2mm. Additional sediment from the same excavation site was collected in the same manner if one large clast weighed more than 20% of the total sample weight.

For the bed armor, I calculated cumulative percent by weight of the bed armor finer than each half-phi interval. The percent finer than a given size was plotted against size for both sediment sampling techniques to determine sediment size distribution (Fig. X); we used this figure to interpolate D_{50} and D_{90} sizes. Using Williams (1983),

$$\omega_{cr} = .0971(D_i)^{1.5} log\left[\frac{1200d}{D_i}\right]$$

where ω_{cr} is the critical stream power to move the particle size (mm) of interest (D_i), and d is the hydraulic radius (m), we calculated the critical stream power to move the D_{50} and D_{90} particles of the armor and bulk sediment at each cross section. In cross sections were bar armor and bulk samples were not collected, we used the average D_{50} and D_{90} values across the reach. We compared necessary stream power for moving each particle size to the modeled stream power at each flow condition and cross section with and without the dam (exported from the HEC-RAS model).

Bank Sediment Analysis

In areas with a muddy bank potentially prone to bank failure after dam removal, we photographed the bank laterally, overlapping images such that one point appears in four different pictures. GPS camera settings and one zoom was used for each bank section; all photographs were taken from mid-channel at approximately the same distance from the bank. Photos were downloaded into Agisoft Metashape to produce a digital model of the banks that could be compared to later models to evaluate changes.

We sampled newly exposed steep, muddy banks to approximate bank strength and susceptibility to erosion. At three cutbanks and one floodplain, we exposed >2 meters of stratigraphy (from just above the water line to the abandoned floodplain). We sampled representative portions of exposed units for hydrometer particle size analysis after Wray 1986.

Approximating bank strength is critical to predict how easily legacy sediments stored in the banks could erode in future flood events. The relationship between silt and clay content of the bank and approximate shear strength was calculated using Julian and Torres (2006),

$$\tau_c = 0.1 + 0.1779(SC\%) + 0.0028(SC\%)^2 - 2.34E - 5(SC\%)^3$$

where *SC%* is the percentage of silt and clay in the sample, measured using hydrometer particle size analysis. The strength of the bank was multiplied by coefficients corresponding to density of vegetated: 1.00 for unvegetated, 1.97 for grass, 5.40 for sparse trees, or 19.20 for dense trees (Julian & Torres 2006). These values for average bank shear strength under different vegetation conditions were compared to shear stress of flow at each cross section within the portion of the reach with steep, muddy banks (Julian & Torres 2006).

To verify whether the material sampled represented historic human-related sedimentation, we conducted radiocarbon dating on multiple dead stumps which grew just above the current water level (revealed by the water level drop following dam removal) (figure 5). We sampled the outer rings of three such dead stumps to determine if the time of their death corresponds with dam construction, which would provide an estimate for prehistoric floodplain height and quantity of legacy sediment accretion. Wood samples were dried at 80 degrees Celsius for 72 hours and cleaned to remove soil, rootlets, insects, or other potential sources of modern carbon. Radiocarbon dating was conducted through DirectAMS. I used Calib704, a radiocarbon dating

calibration program, to determine the potential distribution of ages for the samples given a variable record of C14 production over time in the atmosphere (Stuvier, Reimer, & Reimer 2020). We summed the probability that a deposit was associated with each year multiplied by the year to produce a weighted calibrated age. Weighted calibrated ages better estimate the potential age of the sample and are more stable than using the intercept alone (Telford et al. 2004).

Figure 5. Stumps from trees that grew below the impoundment water level, with roots at current water level. Outer rings of three of these stumps were sampled for radiocarbon dating. The bottom stump is >1-meter-wide and partially filled with cobbles in the interior. This suggests a long period of low water level stability for tree growth and cobble transport after the tree died.

Drone Imagery

To visually document changes to the river resulting from dam removal, we captured aerial imagery and video with drone flights over the study area on five of the seven days of the removal process, including pre-removal, the first day, and the last day (May 23, 24, 25, 29, and 30, 2019). We conducted additional flights on June 4th and July 1st to capture bed structure during a low flow period. Photos were captured with a Mavic 2 Pro camera. 154 photos were captured from 62 meters on May 23rd and 24th. On May 30th, we flew three separate flights over around 3km of the Maury: 200 photos at 68 meters near the dam (repeated on June 4th), 131 photos at 81 meters in the middle of the impoundment, and 124 photos at the same height at the farthest upstream section. On May 25th and 29th and July 1st, we manually captured images of the dam at various low elevations.

Drone photos were imported into Agisoft Metashape to produce a model, DEM, and orthomosaic photo of the flight area. Nine ground control points, geolocated with a Trimble GPS left for 15 minutes at each site, were used to add precision to the geolocation of the model.

Results

Cross sections revealed irregular bed topography. Peaks of relatively high thalweg elevation correspond to shallow riffles (cross sections 1, 7-8, 10, 14, and 16-18) and the remaining sediment ramp behind the removed dam (cross sections 3-4). Remnants of a crib dam near cross section 8, which may have been constructed to power a mill race before the construction of the Jordan's Point dam, could explain the sediment buildup and high elevation in that area. Cross section 14 crosses a mid-channel cobble bar. Cross sections 2, 5, 11-12, and 15 are pools; 2 is the plunge pool which formed beneath the dam. These areas are relatively cobble-poor, with bedrock exposures. Cross sections 15 through 18 are underlain and contained on one side by bedrock ledges, and have a slightly higher slope than the rest of the study area.

In contrast, bank heights throughout the impounded reach are fairly consistent at about half a meter above the low-water level of the impoundment while the dam was in place. Bank height drops about two meters past the crest of the dam. Channel area is highest between cross sections 11 and 15, narrowing in the upstream reach and in the vicinity of the dam (figure 6).

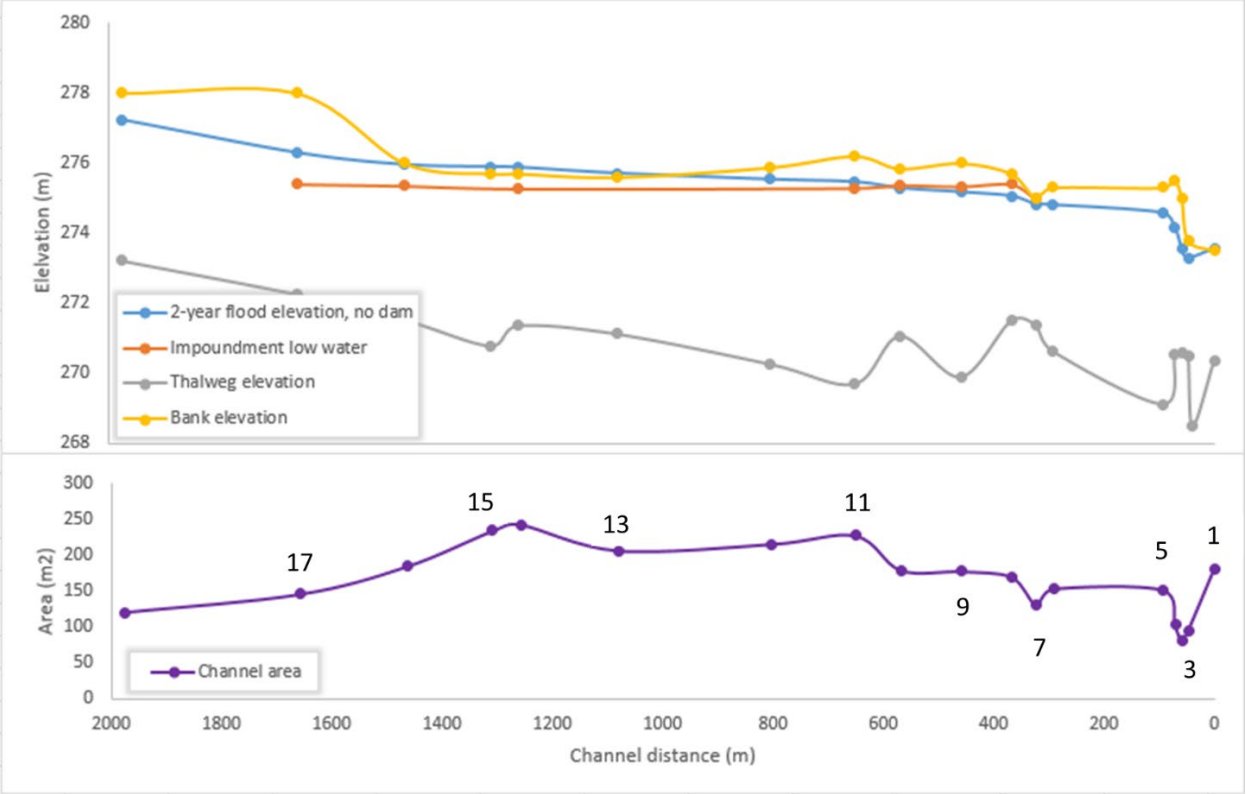

Figure 6. Longitudinal profile of the thalweg, left bank, impoundment low-water line, post-impoundment modeled two-year flood elevation, and two-year-flood cross sectional channel area.

Median (D_{50}) bed armor particles ranged from 23 to 50 mm, and D_{90} bed armor particles ranged from 74 to 150 mm. For the bulk bed material, D_{50} particles ranged from 14 to 23 mm, and D_{90} particles ranged from 53 to 94 mm. There was no clear relationship between particle size and proximity to the dam, although the coarsest material was within the sediment ramp upstream of the dam and at the top of the impoundment (table 2). The bulk sediment is distributed regularly, but the bed armor in all areas sampled exhibits a coarse tail (figure 7).

Table 2. D_{50} and D_{90} particles of the bed armor and bulk sediment based on pebble counts at given cross sections.

	Bed Armor		Bulk Sediment	
Cross sections	*D50*	*D90*	*D50*	*D90*
3-4	40	125	18	85
6-8	40	75	14	53
14-15	32	100	18	60
16	23	74	23	55
17	50	150	20	94

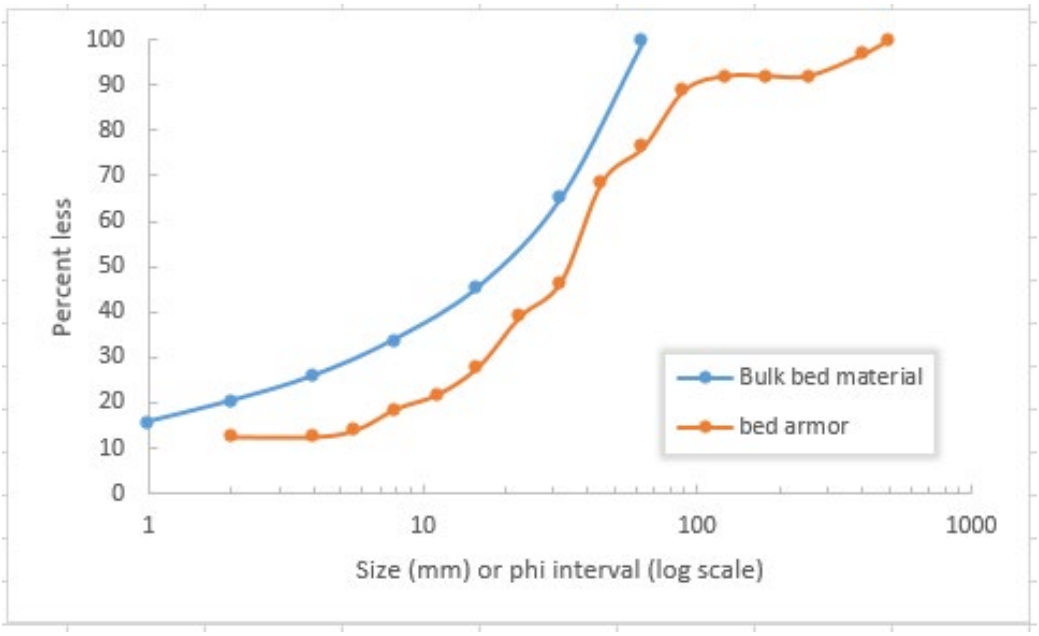

Figure 7. Example sediment size distributions of bar armor and bulk bed samples from cross sections 14 and 15.

Sediment transport capacity is largest near cross section 3 (the remnants of the dam and sediment ramp) and 17 (the top of the impoundment), where slope is steepest and the channel is the most narrow (figure 6). Sediment transport of all but the largest clasts can occur here in almost any flood condition. Smaller sediment transport peaks occur near cross sections 7 and 13; 50- and 100- year floods can move most material here. Without the dam in place, all floods can move median material here as well. In contrast, a 50- or 100-year flood was required to transport

sediment anywhere but above the top of the impoundment and at the dam while the dam was in place. Model results predict that dam removal will result the biggest increases to sediment transport capacity within 500 meters upstream of the dam; D_{90} particles can be moved in even a 2-year flood without the dam, which would have required a 50-year flood while the dam was in place (figure 8).

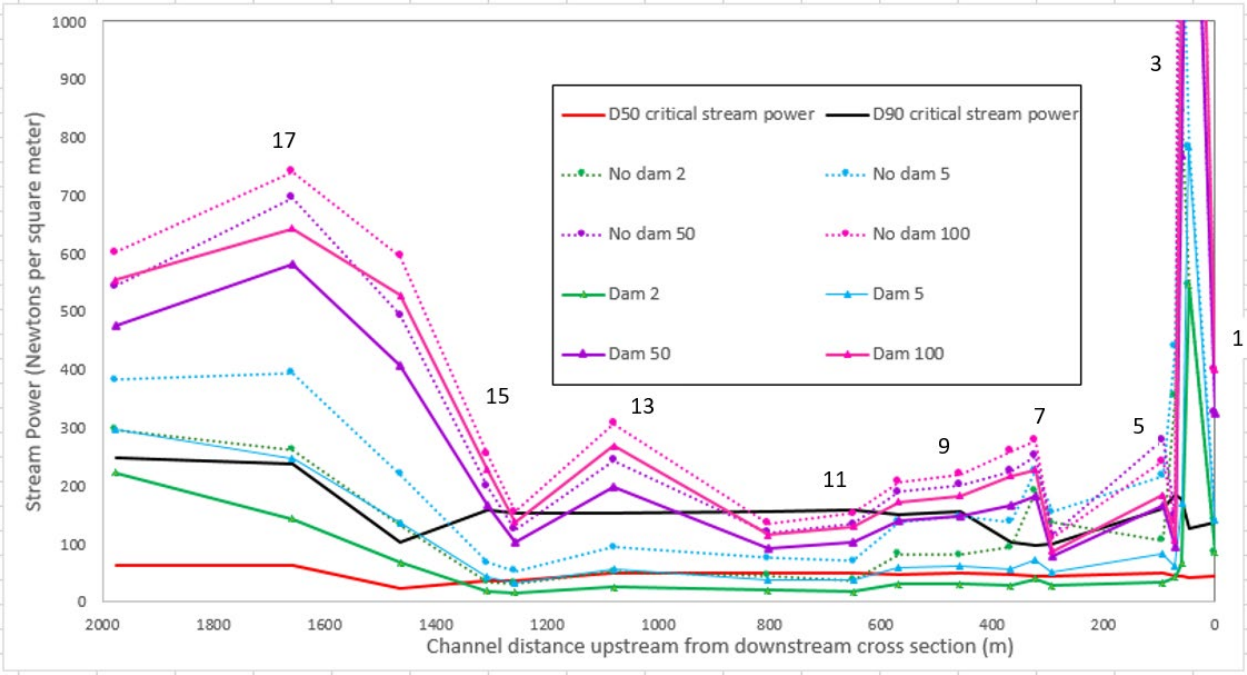

Figure 8. HEC-RAS modeled stream power with and without the dam in place in 2-, 5-, 50-, and 100-year floods from 75 meters below the dam to about 2 kilometers upstream, compared to the critical stream power required to move D_{50} and D_{90} bed armor material.

Bank material, sampled at several locations, was mostly consistent in color and texture both laterally and vertically. We observed minimal layering or soil development and found no evidence of a paleosol (figure 9). Most of the bank material was massive sandy loam with about 70% sand content, although clay content increased below the impoundment low-water level (table 3). We calculated the shear strength of the predominant bank material if left bare, planted with grasses, stabilized with trees, or stabilized with dense trees in the area with the most exposed steep, muddy bank material (between cross sections 7 and 12). Shear stress of flow exceeds shear strength of bare or grassy banks in all floods in this region, and of sparse tree-

covered banks in greater than a five-year flood for cross sections 7 to 10. Dense tree cover strengthens banks enough to far exceed the shear stress of even a 100-year flood (figure 10).

Figure 9. An exposure of uniform fine-grained bank material.

Table 3. Field soil texture and hydrometric analysis results of representative samples of bank sediment.

Sample depth	Texture	% clay	% silt	% sand
2m	Sandy loam	25	5	70
>2m	Sandy clay loam	35	15	50

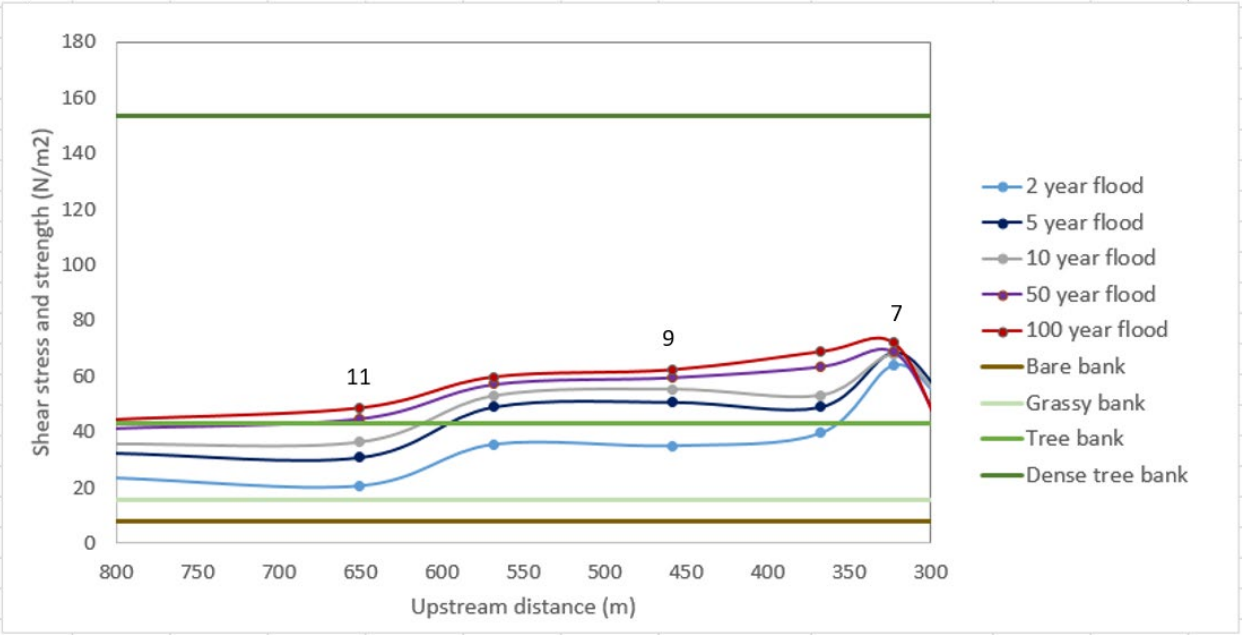

Figure 10. Shear strength of the banks with varying levels of vegetation reinforcement, compared to shear stress applied by floods modeled in HEC-RAS between cross sections seven and twelve.

Death ages of the stumps growing at the current water level ranged from 1754 to 1778 with an error of 25 to 34 years. Uniform bank material, 2.67 to 3.86 meters in height above the stumps, was likely deposited after this time, resulting in an average deposition rate since the mid-18th century along the reach ranging from 11 to 16 mm/yr. (table 4).

Table 4. Calibrated death ages of sampled stumps, their respective bank heights, and their minimum average deposition rates since the mid-1700s.

Sample	Calibrated radiocarbon age (yr)	1σ error	Bank height (m)	Average deposition rate (mm/yr)
Iosso1	1769	25	2.67	11
Iosso2	1754	34	3.53	13
Iosso3	1778	26	3.86	16

Discussion

Studying and modeling the implications of the construction and removal of the Jordan's Point Dam provide insight into similar low-head dams with minimal fine sediment storage in the channel. We evaluate the impact of the dam on the Maury River using a combination of field measurements and modeling. The largest impacts of construction of the dam were to cobble mobility and floodplain heights, where large amounts of legacy sediments are stored. These factors have consequences for channel evolution in future floods following dam removal, by altering stream power, influencing bedload mobility, and producing risks for the erosion of legacy sediment.

Distribution of channel sediment and modeling provides evidence for changes in sediment transport while the dam was in place. Like previous studies documenting a coarsening of the bed behind the dam (Skalak, Pizzuto, & Hart 2009), we observed a coarse tail on the distribution of bed armor (figure 7). This coarsening is most evident at the dam and at the top of the impoundment, where finer material continued to be transported while coarse material was deposited (table 2). Pearson and Pizzuto (2015) document transport of gravels and fine cobbles over low-head dams, which may have occurred on the Maury River to produce the observed distribution, leaving disproportionately large material behind. Moreover, model results support this possibility as median particles could move through the impounded reach in as little as a five-year flood, and a 50-year flood or greater could move all material in the stream. One of the stumps that died in 1700s was internally hollowed out with large cobbles inside, which indicates that these larger than median-sized cobbles moved after the tree died and while the dam was in place (figure 5). Combined, this evidence clearly indicates that particles much smaller than the median particle (sand and gravels) moved over the dam easily in floods, and coarser material built the bar and pool structure observed upstream of the dam.

As a low-head dam, it is unlikely that major changes to channel morphology beyond the channel bed occurred while the dam was in place. Bed structure such as the sediment ramp and plunge pool beneath the dam (cross sections 3-4 and 2, respectively, figure 6) likely were created by the dam. Similarly, the higher bed elevations at cross section 8 may be a sediment ramp from the remnants of the crib dam. Pool-riffle sequences, such as the extended pool between cross sections 11 and 13, exposed by dam removal could have been formed during the 200-year presence of the dam, due to the ability of most cobbles to move in 50-year flood (figure 9). However, due to the lack of historical imagery of the Maury River from before the mid-20th century, more than 100 years after the dam was first constructed, the pre-dam channel geometry is largely unknown.

While the dam was in place, overbank flooding resulted in steady floodplain deposition and accretion of legacy sediments. Deposition of sandy material on the right and left floodplains was locally common in the years immediately before dam removal, but flow since its removal has yet to top the banks in the impounded reach. The floodplain could be inundated in a two-year flood with the dam (figure 4), suggesting floodplains were active. The lack of soil development in the floodplains supports the idea that floodplains were being actively flooded until the removal of the dam. Two main pieces of evidence characterize bank sediment as legacy sediment along the Maury River. Floodplain sediments were uniform and lacked soil development or horizonation both near and far from the channel (figure 9, table 3). Although the initial channel geometry is unknown, this suggests at least 3 meters of sediments have accreted through a large area of the river corridor. Secondly, the radiocarbon death ages of sampled stumps all correspond to the mid-1700s, likely a time where the water level rose and drowned the trees (table 3). Their large diameter and consistent age and height above the post-dam water level suggest that they may have been growing on the pre-European settlement and pre-dam floodplain or bar or at least a surface that was stable for a long period of time to allow uninterrupted tree growth. Modern sycamores grow both on the floodplain and on cobble bars build by low-frequency floods below the modern floodplain. Death ages of sampled stumps correspond with the founding of Lexington and the increase of broad agricultural activity in the watershed (“Lexington”). The dates are before first record of the Jordan’s Point Dam, but this may be due to lost tree rings or earlier dams in the area (like the crib dam at cross section 8). Further, water level and discharge changes could have occurred earlier due to deforestation or agricultural activity (Magilligan &

Stamp 1997). Even if the timing and cause of death are uncertain, these tree stumps provide evidence to suggest three or more meters of legacy sediments have deposited since the late 1700s, at a rate of approximately 13 mm/yr. In a similar study by Pizzuto et al. (2016) on another Virginia stream in the valley and ridge province with extensive damming, sedimentation rates in the 20th century ranged from 8 to 50 mm/year, in contrast to previous centuries of early European settlement where deposition rates were higher, near 50 to 200mm/year. Our rates are low but within the observed rates in previous, similarly located studies, and the long period of consistent impoundment has resulted a thick legacy sediment package.

Since the dam removal, low-flow conditions and floods that have not exceeded the height of the bank have resulted in mobility of sand, at minimum, throughout the reach, and some erosion of the exposed muddy banks. However, modeling informs future changes. We predict these changes will include lower flood heights, sediment transport, and bank erosion, potentially coupled with bar building. Following dam removal, a five-year or greater flood is required to inundate the floodplains. This channelized flow increases stream power and shear stress, which in turn mobilize sediment on the bed and erode banks. Given that bed armor can easily be transported by moderate frequency flooding, smaller bulk material underneath will be quickly excavated (figure 8) and bar building, erosion and/or lateral shifting will likely occur. However, a 50-year flood may be required to cause major channel changes.

The potential harm such bedload transport can do is illustrated by a case further downstream. Following removal of the Balcony Falls dam on the James River near the Maury River confluence in 1974, dramatic growth of cobble bars at the head of the dam was matched by significant erosion of legacy sediments from the opposite bank between 2003 and 2014 (figure 11), releasing approximately 702 tons of sediment per year into rivers draining in the Chesapeake Bay (“Maury River Stream Restoration” 2016). The Maury River may evolve similarly in the area of the Jordan’s Point Dam now that cobbles can easily be mobilized in the channelized reach immediately upstream of the dam.

Figure 11. Severe bank erosion in 2003 on the Maury River (downstream of Jordan's Point) due to bar migration and growth following a dam removal in 1974 (photo credit: Virginia Department of Transportation).

Moving cobble collisions with the banks could threaten bank stability and lead to spectacular bank erosion, which is particularly concerning due to the documented legacy sediments. Shear stress of flow without moving cobbles in anything more than a two-year flood may erode legacy sediment of the banks if left unvegetated; only heavily tree-stabilized banks have sufficient shear strength to mitigate bank erosion (figure 10). The preliminary bank stabilization measure employed was planting grasses, but this solution was insufficient to protect from the shear stress of even a two-year flood. Upstream portions of the study area are more covered with natural vegetation and trees, and so will be able to better withstand erosive forces. However, floodplains and banks closer to the dam are mostly grassy with sparse trees (yards and parks), with more surrounding infrastructure (homes, roads, bridges, etc.). Despite only minor flooding, bank

erosion is already occurring especially near cross section 7 (figure 12) where the modeled shear stress peaks locally (figure 10). High banks in this reach will likely require further stabilization. Even dense tree stabilization may be insufficient to resist shear stress applied by moving cobbles in flood events as bars build.

Figure 12. Channel migration into the left bank, resulting in bank erosion at cross section 7 (photo taken December 2019). Most of this discarded debris predates the removal of the dam where the impounded reach suffered erosion in high flows along the outside of a bend. Nonetheless, bank erosion is ongoing following dam removal.

Conclusion

The removal of the Jordan's Point Dam on the Maury River provided an ideal case study to characterize the past impacts of the dam on channel morphology and sediment transport and storage, and model the future effects of its removal. As a low-head dam with little fine sediment storage behind it, the impacts of its removal are relevant to many other future dam removals. While the dam was in place for more than 200 years, several meters of legacy sediments accreted in the floodplains at a rate of 13 mm/yr. Cobbles moved through the impoundment and over the dam in high magnitude floods, which may have produced the bedforms exposed by dam removal. Following dam removal, modeling predicts that these heightened floodplains will

channelize flow, increasing stream power and cobble mobility. Without bank stabilization, impacts with moving cobbles may severely erode legacy sediments in the banks.

Future research on the Jordan's Point Dam is required to fully characterize the impact of its removal. River responses to dam removals can last years or decades (Kim & Toda 2018). In order to completely understand the impact of the dam removal, cross sections and drone flights should be repeated after future flood events, particularly those capable of moving most bed materials (50+ year recurrence). Measuring future changes and comparing them to model results will evaluate the effectiveness of this approach of river characterization and 2D modeling as a tool to predict threats to infrastructure and sediment pollution. Additionally, repeat surveys would increase general understanding of the long-term consequences of low-head dam removal in an area such as the Maury River with abundant aging dams that will eventually require removal. Another method to increase understanding of how dam removals control sediment transport mechanics with increased granularity is RFID-tagging cobbles and tracking their movement in future flood events.

Acknowledgements

This research was generously funded by the Washington and Lee Geology Department through the Ed Spencer Award. We would like to thank David Pfaff for his drone and technology expertise and Iszak Morgan for his assistance in the field. Thank you to Washington and Lee Special Collections for finding historical records and imagery of the dam. We are grateful to the landowners that allowed us access to their property. Finally, thank you to Louise Finger for her invaluable insight on this and previous dam removals.

References

Arcement, G., & Shneider, V. (1989). *Guide for selecting Manning's roughness coefficients for natural channels and flood plains* (USGS Water Supply Paper No. 2339). https://doi.org/10.3133/wsp2339

Barnes, H. H. (1967). *Roughness Characteristics of Natural Channels*. U.S. Government Printing Office.

Burroughs, B. A., Hayes, D. B., Klomp, K. D., Hansen, J. F., & Mistak, J. (2009). Effects of Stronach Dam removal on fluvial geomorphology in the Pine River, Michigan, United States. *Geomorphology*, 96-107.

Cannatelli, K. M. & Curran, J. C. (2012). Importance of hydrology on channel evolution following dam removal: case study and conceptual model. *Journal of Hydraulic Engineering*, 377-390.

Casserly, C. M., Turner, J. N., O'Sullivan, J. J., Bruen, M., Bullock, C., Atkinson, S., & Kelly-Quinn, M. (2020). Impact of low-head dams on bedload transport rates in coarse-bedded streams. *Science of The Total Environment*, *716*, 136908. https://doi.org/10.1016/j.scitotenv.2020.136908

DGIF (VA Dept. of Game & Inland Fisheries). (2018). Environmental Assessment: Jordan's Point Dam Removal, Maury River, City of Lexington and Rockbridge Co., VA, 79p, available from http://lexingtonva.gov/gov/projects/jordans_point_dam.htm

England, J.F., Jr., Cohn, T.A., Faber, B.A., Stedinger, J.R., Thomas, W.O., Jr., Veilleux, A.G., Kiang, J.E., and Mason, R.R., Jr., 2019, Guidelines for determining flood flow frequency—Bulletin 17C (ver. 1.1, May 2019): U.S. Geological Survey Techniques and Methods, book 4, chap. B5, 148 p., https://doi.org/10.3133/tm4B5.

Fencl, J. S., Mather, M. E., Costigan, K. H., & Daniels, M. D. (2015). How Big of an Effect Do Small Dams Have? Using Geomorphological Footprints to Quantify Spatial Impact of Low-Head Dams and Identify Patterns of Across-Dam Variation. *PLOS ONE*, *10*(11), e0141210. https://doi.org/10.1371/journal.pone.0141210

Gartner, J. D., Magilligan, F. J., & Renshaw, C. E. (2015). Predicting the type, location and magnitude of geomorphic responses to dam removal: Role of hydrologic and geomorphic constraints. *Geomorphology,* 20-30.

Gerald P Wilkes, Spencer, E., Nick H Evans, & Elizabeth M Campbell. (2007). Geology of Rockbridge County, Virginia. *170*, 64.

HEC-RAS Downloads. (n.d.). Retrieved April 14, 2020, from https://www.hec.usace.army.mil/software/hec-ras/download.aspx

Hupp, C. R., Schenk, E. R., Kroes, D. E., Willard, D. A., Townsend, P. A., & Peet, R. K. (2015). Patterns of floodplain sediment deposition along the regulated lower Roanoke River, North Carolina: Annual, decadal, centennial scales. *Geomorphology*, *228*, 666–680. https://doi.org/10.1016/j.geomorph.2014.10.023

Hupp, Cliff R., Noe, G. B., Schenk, E. R., & Benthem, A. J. (2013). Recent and historic sediment dynamics along Difficult Run, a suburban Virginia Piedmont stream. *Geomorphology*, *180–181*, 156–169. https://doi.org/10.1016/j.geomorph.2012.10.007

Julian, J. & Torres, R. (2006). Hydraulic erosion of cohesive riverbanks. *Geomorphology*, 76, 193-206. 10.1016/j.geomorph.2005.11.003.

Kalbian, M., & Pezzoni, J. (2019). *Removal report on Jordan's Point concrete dam and timber crib dam : May 23-25, and May 28-30, 2019.*

Kim, S. & Toda, Y. (2018). Effects of influential parameters on long-term channel evolution following low-head dam construction and removal. *Journal of Water Resource and Protection*, *10,* 780-793.

Lexington | Virginia, United States. (n.d.). Encyclopedia Britannica. Retrieved April 16, 2020, from https://www.britannica.com/place/Lexington-Virginia

Magilligan, F. J., & Stamp, M. L. (1997). Historical Land-Cover Changes and Hydrogeomorphic Adjustment in a Small Georgia Watershed. *Annals of the Association of American Geographers*, *87*(4), 614–635. https://doi.org/10.1111/1467-8306.00070

OSU Streamflow Tutorial—Flood Analysis Tutorial with Daily Data (Log-Pearson Type III Distribution). (n.d.). Retrieved February 14, 2020, from https://streamflow.engr.oregonstate.edu/analysis/floodfreq/meandaily_tutorial.htm

Pearson, A. J., & Pizzuto, J. (2015). Bedload transport over run-of-river dams, Delaware, U.S.A. *Geomorphology*, *248*, 382–395. https://doi.org/10.1016/j.geomorph.2015.07.025

Peeters, A., Houbrechts, G., Hallot, E., Van Campenhout, J., Gob, F., & Petit, F. (2020). Can coarse bedload pass through weirs? *Geomorphology*, *359*, 107131. https://doi.org/10.1016/j.geomorph.2020.107131

Pizzuto, J. (2002). Effects of dam removal on river form and process. *BioScience 52*(8), 683-691.

Roberts, S. J., Gottgens, J. F., Spongberg, A. L., Evans, J. E., & Levine, N. S. (2007). Assessing Potential Removal of Low-Head Dams in Urban Settings: An Example from the Ottawa River, NW Ohio. *Environmental Management*, *39*(1), 113–124. https://doi.org/10.1007/s00267-005-0091-8

Skalak, K., Pizzuto, J., & Hart, D. D. (2009). Influence of Small Dams on Downstream Channel Characteristics in Pennsylvania and Maryland: Implications for the Long-Term Geomorphic Effects of Dam Removal1. *JAWRA Journal of the American Water Resources Association*, *45*(1), 97–109. https://doi.org/10.1111/j.1752-1688.2008.00263.x

Stuiver, M., Reimer, P.J., and Reimer, R.W., 2020, CALIB 7.1 [WWW program] at http://calib.org, accessed 2020-3-11

StreamStats. (n.d.). Retrieved April 13, 2020, from https://streamstats.usgs.gov/ss/

Telford, R. J., et al. (2004). "The intercept is a poor estimate of a calibrated radiocarbon age." *The Holocene* 14(2): 296-298.

Trout, W. (1991). *The Maury River atlas : nineteenth-century inland navigations of the Virginias* . Lexington, Va: The Canals and Navigation Society.

Maury River Stream Restoration II at Echols Farms, Glasgow, VA. (2016). US Army Corps of Engineers Norfolk District Regulatory Office.

USGS. (2020). 3D Elevation Program, https://www.usgs.gov/core-science-systems/ngp/3dep, obtained from the VA Dept Mines Mineral and Energy, March 2020. 1 m grid.

Wickline, A. (2018, September 28). *Rockbridge County faces flooding issues after heavy overnight rains*. https://www.wsls.com/news/2018/09/28/rockbridge-county-faces-flooding-issues-after-heavy-overnight-rains/

Wildman, L. A. S., & MacBroom, J. G. (2005). The evolution of gravel bed channels after dam removal: Case study of the Anaconda and Union City Dam removals. *Geomorphology*, *71*(1–2), 245–262. https://doi.org/10.1016/j.geomorph.2004.08.018

Williams, G. (1983). Paleohydrological Methods and Some Examples from Swedish Fluvial Environments. I. Cobble and Boulder Deposits. Geografiska Annaler. Series A, Physical Geography. 65. 227. 10.2307/520588.

Wray, W. K. (1986). *Measuring engineering properties of soil*. Prentice-Hall.